



Structure-based de novo design and biochemical evaluation of novel Cdc25 phosphatase inhibitors

Hwangseo Park^{a,*}, Young Jae Bahn^b, Seong Eon Ryu^{b,*,†}

^a Department of Bioscience and Biotechnology, Sejong University, 98 Kunja-dong, Kwangjin-ku, Seoul 143-747, Republic of Korea

^b Systemic Proteomics Research Center, Korea Research Institute of Bioscience and Biotechnology, 52 Eoeun-dong, Yuseong-gu, Daejeon 305-333, Republic of Korea

ARTICLE INFO

Article history:

Received 6 April 2009

Accepted 20 May 2009

Available online 27 May 2009

Keywords:

Cdc25 phosphatase

De novo design

Docking

Anticancer agents

ABSTRACT

Cdc25 phosphatases have been considered as attractive drug targets for anticancer therapy due to the correlation of their overexpression with a wide variety of cancers. We have been able to identify 32 novel Cdc25 phosphatase inhibitors with micromolar activity by means of a structure-based de novo design method with the two known inhibitor scaffolds. Because the newly discovered inhibitors are structurally diverse and have desirable physicochemical properties as a drug candidate, they deserve further investigation as anticancer drugs. The differences in binding modes of the identified inhibitors in the active sites of Cdc25A and B are addressed in detail.

© 2009 Elsevier Ltd. All rights reserved.

Cdc25 phosphatases are able to dephosphorylate both threonine and tyrosine side chains of a protein substrate, and therefore belong to a class of dual-specificity phosphatase. Of the three Cdc25 homologues (Cdc25A, Cdc25B, and Cdc25C) encoded in human genome, Cdc25A and Cdc25B are shown to have oncogenic properties.¹ Cdc25A acts on the control of G₁-to-S and G₂-to-S transitions in cell cycle whereas Cdc25B is mainly responsible for regulating the progression at the G₂-to-M transition.² Cdc25 phosphatases can thus serve as the central regulators of the cell cycle with the role of driving each state of cell division. So far, several lines of experimental evidence have been provided for the involvement of Cdc25 phosphatases in oncogenic transformations and various human cancers.^{3–6} The inhibition of Cdc25 phosphatases may thus represent a novel approach for the development of anticancer therapeutics.

Structural studies of Cdc25 phosphatases have lagged behind the mechanistic and pharmacological studies. The X-ray crystal structures of the catalytic domains of Cdc25A and B have been reported so far in their ligand-free forms only.^{7,8} The lack of structural information about the nature of the interactions between Cdc25 phosphatases and small molecule inhibitors has made it a difficult task to discover a good lead compound for anticancer drugs. Nonetheless, a number of effective inhibitors of Cdc25 phos-

phatases have been discovered with structural diversity as recently reviewed in a comprehensive manner.^{9,10} Most of the Cdc25 inhibitors reported in the literature have stemmed from either the isolation of new scaffolds by high throughput screening¹¹ or the generation of the improved derivatives of pre-existing inhibitor scaffolds.^{12–14} Binding modes of the newly found Cdc25 inhibitors have also been addressed with docking simulations in the active site to gain structural insight into their inhibitory mechanisms.^{15–17}

Recently, we have identified several novel classes of Cdc25 phosphatase inhibitors with micromolar activity based on the structure-based virtual screening with docking simulations.¹⁸ Most of these new inhibitors proved to be competitive in their respective Lineweaver–Burk plots and could be categorized into the two scaffolds, **1** (5-methylene-2-phenylamino-thiazol-4-one) and **2** (1-phenyl-2-(4H-[1,2,4]triazole-3-ylsulfanyl)-ethanone) as shown in Figure 1. In present study, we apply a de novo design approach to find the derivatives of the two inhibitor scaffolds that have an improved inhibitory activity with good physicochemical properties as a drug candidate. The characteristic feature that discriminates our de novo design approach from the others lies in the implemen-

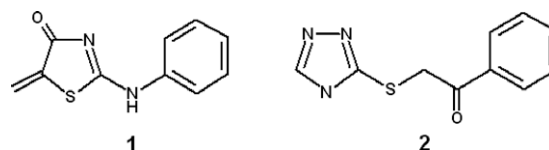
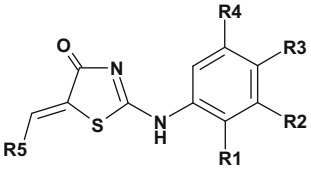


Figure 1. Chemical structures of the two inhibitor scaffolds under investigation.

* Corresponding authors. Tel.: +82 2 3408 3766; fax: +82 2 3408 4334 (H.P.); tel.: +82 42 860 4149; fax: +82 42 860 4598 (S.E.R.).

E-mail addresses: hspark@sejong.ac.kr (H. Park), ryuse@kribb.ac.kr, ryuse@hanyang.ac.kr (S.E. Ryu).

† Present address: Department of Bio Engineering, Hanyang University, 17 Haengdang-dong, Seongdong-gu, Seoul 133-791, Republic of Korea. Tel.: +82 2 2220 2349; fax: +82 2 2220 0521.

Table 1
Structures and inhibitory activities of the derivatives of **1**


	R1	R2	R3	R4	R5 ^a	IC ₅₀ (μM)	
						Cdc25A	Cdc25B
1a	H	H	Cl	H		15.4	3.1
1b	H	H	F	H		14.3	3.7
1c	H	Br	H	H		7.7	2.7
1d	H	Cl	H	H		9.1	3.2
1e	H	Cl	H	Cl		5.1	1.2
1f	H	Me	Me	H		7.1	1.8
1g	Cl	H	H	H		10.1	2.1
1h	Cl	Cl	H	H		6.2	2.1
1i	H	H	F	H		30.7	8.9
1j	H	Cl	H	H		12.8	3.3
1k	H	Me	Me	H		8.1	2.3
1l	H	Cl	H	H		11.1	4.4
1m	H	H	Br	H		17.3	5.1
1n	H	Cl	H	Cl		4.1	2.3
1o	H	OH	H	H		7.8	2.8

Table 1 (continued)

	R1	R2	R3	R4	R5 ^a	IC ₅₀ (μM)	
						Cdc25A	Cdc25B
1p	Cl	H	Cl	H		6.7	4.5
1q	H	Cl	H	Cl		12.7	2.3
1r	Cl	H	Cl	H		12.6	2.6
1s	Cl	H	H	H		10.3	3.9

^a Asterisk indicates the atom attached to the position of substitution.

tation of an accurate solvation model in calculating the binding free energy between Cdc25 phosphatases and the putative inhibitors, which would have an effect of increasing the accuracy in predicting the binding affinity.¹⁹ On the basis of docking simulations, we will also address the interactions of the newly identified inhibitors with the active site residues of Cdc25 phosphatases.

LigBuilder program²⁰ was used in the structure-based de novo design of Cdc25 phosphatase inhibitors using the crystal structure of Cdc25B (PDB entry: 1cwr).⁸ In order to score the derivatives according to the relative binding affinity, the program employs the empirical binding free energy function including van der Waals, hydrogen bond, electrostatic, and entropic terms.²¹ Gasteger–Marsilli atomic charges²² were used for both proteins and ligands in the calculation of the electrostatic interaction term. The current scoring function of LigBuilder lacks a solvation term although the effects of ligand solvation have been shown to be critically important in protein–ligand interactions.¹⁹ Therefore, the solvation free energy function developed by Kang et al.²³ was added to improve the original scoring function. The two inhibitor scaffolds identified in the virtual screening (**1** and **2** in Fig. 1) were used as the starting structures of de novo design. The first step to design the new derivatives was to analyze the binding pocket of the active site using the POCKET module. The structures of Cdc25B in complex with **1** and **2** obtained from docking simulations with the AUTODOCK program²⁴ were used as input for POCKET to find the key interaction residues in the active site. The next step involves the generation of the derivatives of the two inhibitor scaffolds by applying the genetic algorithm as implemented in the GROW module. The bioavailability rules were also applied to screen the derivatives with good physicochemical properties as a drug.²⁵

The catalytic domains of the two Cdc25 phosphatases (Cdc25A: residues 336–523; Cdc25B: residues 378–566)²⁶ were overexpressed in *Escherichia coli* by using pET28a (Novagen) with 6xHis tag in the N-terminus. The overexpressed Cdc25 phosphatases were purified by Ni-NTA affinity resin (Qiagen) and frozen (–75 °C) in a buffer of pH 8.0 containing 20 mM Tris–HCl, 0.2 M NaCl, and 5 mM DTT until enzyme assay. In the phosphatase assay using 96 well plates, the reaction mixture included 180 μl of reaction buffer (20 mM Tris–HCl, 0.01% Triton X-100, and 5 mM DTT) with 10 μM 6,8-difluoro-4-methylumbelliferyl phosphate (DiFMUP, molecular probe), 10 μl of enzyme (30 nM Cdc25A or 20 nM Cdc25B), and 10 μl of a designed putative inhibitor dissolved in DMSO. The reaction was performed for 20 min at room temperature and stopped by adding 1 mM sodium orthovanadate (final

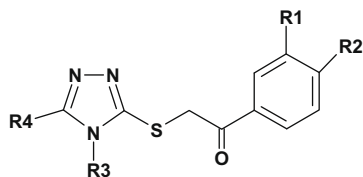
concentration). The fluorescence was measured (355 nm excitation and 460 nm emission) by a plate reader. IC₅₀ values were then estimated at least three times and the averaged values were selected. As the positive controls for the enzyme inhibition assay, we used the Cdc25 phosphatase inhibitor known as NSC 95397. This compound has micromolar inhibitory activity against Cdc25 phosphatase

and are known to be one of the most potent growth inhibitors of various tumor cell lines.^{27,28} The IC₅₀ values of NSC 95397 were found to be 5.5 and 19.2 μM for Cdc25A and Cdc25B, respectively, in the present enzyme assay.

In the present structure-based de novo design study, we explore the substituent space on the two promising cores at four or five

Table 2

Structure and inhibitory activity of the derivatives of **2**



	R1	R2 ^a	R3 ^a	R4 ^a	IC ₅₀ (μM)	
					Cdc25A	Cdc25B
2a	OH	OH			6.0	1.7
2b	OH	OH			9.2	4.7
2c	H	NO ₂	Me		19.0	5.4
2d	H		Me		13.1	4.2
2e	Cl	Cl			11.4	6.9
2f	OH	OH			7.1	2.6
2g	H		Me		13.0	2.0
2h	H	Cl			14.5	5.2
2i	H	Cl	Et		17.2	6.0
2j	OH	OH			7.1	2.5
2k	OH	OH			4.7	2.3
2l	OH	OH			11.5	1.6
2m	H	NO ₂	Me		11.1	4.4

^a Asterisk indicates the atom attached to the position of substitution.

positions to identify the substituents that can enhance the inhibitory activity against Cdc25 phosphatases with the desirable physicochemical properties as a drug candidate. This de novo design was operated by varying the substituents to optimize the binding free energy with the core structure being kept fixed. Structures were evolved from the hydrogens attached to the molecular cores as the substitution points. For each of the two scaffolds, 10,000 derivatives were generated and scored according to the calculated binding affinities. The top-scored 500 molecules for each scaffold were then checked for commercial availability. Finally, 107 and 82 derivatives of **1** and **2** were respectively purchased from compound suppliers and tested for inhibitory activities against Cdc25A and B.

Of the 107 derivatives of **1** tested for the inhibitory activities, 19 were found to have IC_{50} values less than $10\text{ }\mu\text{M}$ for at least one of the two Cdc25 phosphatases. Table 1 lists the structures and IC_{50} values of the newly found inhibitors. We note that most of the derivatives exhibit a higher inhibitory activity for Cdc25B than for Cdc25A. This is not surprising because the structure-based de novo design was carried out using the 3-D structure of Cdc25B. It is also noteworthy that halogen atoms and methyl groups appear to be suitable substituents on the phenyl ring of **1**. Judging from the presence in all derivatives, a chemical group involving an aromatic ring at the terminal R5 position seems to be indispensable for the micromolar inhibitory activity. All of the inhibitors shown in Table 1 satisfy the Lipinski's 'Rule of Five' for physicochemical properties as a drug candidate,²⁵ indicating that they deserve further investigation as an anticancer drug.

Thirteen derivatives of **2** exhibited the IC_{50} values less than $10\text{ }\mu\text{M}$ for at least one of the two Cdc25 phosphatases, whose structures and IC_{50} values are listed in Table 2. As in the case of scaffold **1**, most of the derivatives exhibit a higher inhibitory activity for Cdc25B than for Cdc25A. It is also a similar structural feature to scaffold **1** that only the large substituents with an aromatic ring are allowed at R4 position of the terminal triazole group of **2**. However, scaffold **2** differs from **1** in that not only the derivatives with small substituents but also those with a bulky group such as the phenyl ring at R2 position may be a potent inhibitor of Cdc25 phosphatases (See **2d** and **2g** in Table 2 for example). The two hydroxyl substituents at the terminal phenyl ring seem to be important in

particular for the inhibition of Cdc25A because most of the derivatives with hydroxyl moieties at R1 and R2 positions have IC_{50} values less than $10\text{ }\mu\text{M}$ against Cdc25A.

To obtain some energetic and structural insight into the inhibitory mechanisms by the newly identified inhibitors of Cdc25 phosphatases, their binding modes in the active sites of Cdc25A and B were investigated using the AUTODOCK program.²⁴ The calculated binding modes of the most potent inhibitor (**1e**) among the derivatives of scaffold **1** are compared in Figure 2. A substantial difference in binding mode is observed in the pattern for the formation of hydrogen bonds: the thiazol-4-one ring of **1e** receives two hydrogen bonds from the backbone amidic nitrogen atoms in the active site of Cdc25B whereas the roles of hydrogen bond donors with respect to the inhibitor thiazol-4-one moiety are played by the side-chain guanidium group of Arg436 in the active of Cdc25A. We note that the phenyl ring of **1e** resides at the entrance of active site in the Cdc25A–**1e** complex. On the other hand, it is situated deep in the active site of Cdc25B, establishing a hydrophobic contact with the side chains of Tyr428, Arg479, and Met531. These structural features are consistent with a higher inhibitory activity of **1e** for Cdc25B than Cdc25A. Thus, the involvement of stronger hydrophobic interactions in the Cdc25B–**1e** complex than in the Cdc25A–**1e** one can be an explanation for the differences in IC_{50} values of the derivatives of scaffold **1** for the two Cdc25 phosphatases.

Figure 3 compares the calculated binding modes in the active sites of the two Cdc25 phosphatases for the most potent inhibitor (**2k**) among the derivatives of scaffold **2**. It is common to the two binding configurations that one of the nitrogen atoms on the inhibitor triazole ring forms a hydrogen bond with the side-chain guanidium group of the Arg residue around the active site (Arg436 in Cdc25A and Arg479 in Cdc25B). Judging from the proximity to the Arg residues in the active site, the triazole moiety may serve as a surrogate for the phosphate group of the substrate for Cdc25 phosphatases. The large differences in binding modes between Cdc25A–**2k** and Cdc25B–**2k** complexes are observed in the pattern for the formation of hydrogen bonds. Both phenolic oxygens of **2k** form three hydrogen bonds with the backbone amidic nitrogen atoms and the side chain of Cys430 in the Cdc25A–**2k** complex. In contrast, only one of the two phenolic oxygens is involved in a bifurcated hydrogen bond with the side-chain carboxylate groups of the two Glu residues

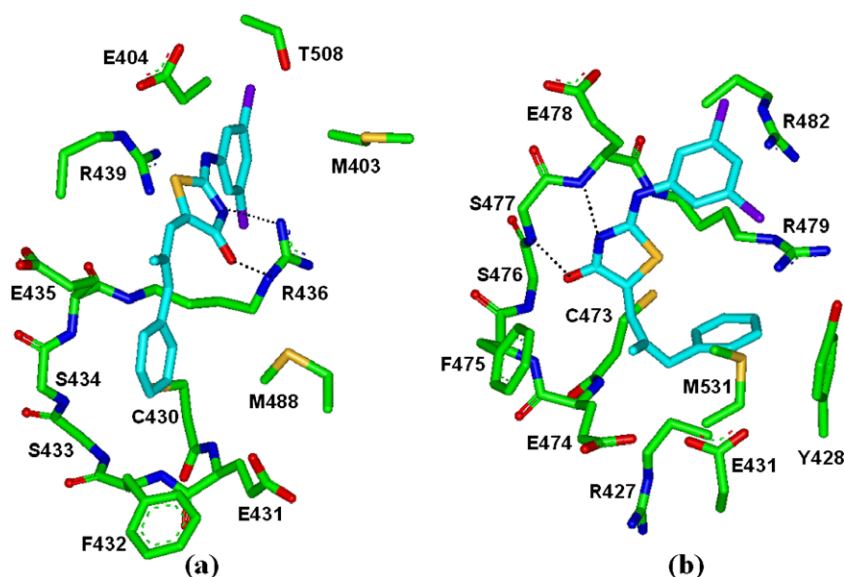


Figure 2. Calculated binding modes of **1e** in the active sites of (a) Cdc25A and (b) Cdc25B. Carbon atoms of the protein and the ligand are indicated in green and cyan, respectively. Each dotted line indicates a hydrogen bond.

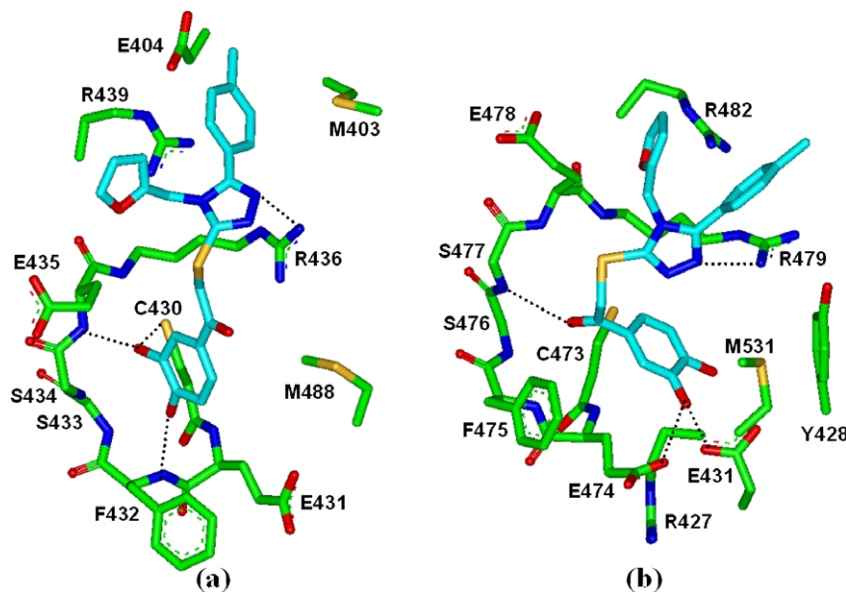


Figure 3. Calculated binding modes of **2k** in the active sites of (a) Cdc25A and (b) Cdc25B. Carbon atoms of the protein and the ligand are indicated in green and cyan, respectively. Each dotted line indicates a hydrogen bond.

(Glu431 and Glu474) in the active site of Cdc25B. The presence of multiple hydrogen bonds in the two active sites indicates that the dihydroxyphenyl moiety can play a role of anchor for binding of **2k** in the active sites of Cdc25 phosphatases. It is also noteworthy that the carbonyl oxygen of **2k** receives a hydrogen bond from a backbone amide group of Cdc25B whereas it is exposed to bulk solvent in Cdc25A–**2k** complex. This difference may be invoked to explain a little higher inhibitory activity of **2k** for Cdc25B than for Cdc25A. The dihydroxyphenyl group of the inhibitor resides in the vicinity of non-polar residues in the active sites of Cdc25 phosphatases: Phe432 and Met488 for Cdc25A, and Tyr428 and Met531 for Cdc25B. This indicates that, as in the case of **1e**, hydrophobic interactions should also be a significant binding force stabilizing **2k** in the active sites of Cdc25 phosphatases.

The difference in binding modes of the inhibitors in the active sites of the two Cdc25 phosphatases can be attributed to the difference in active site geometry. In this regard, the volume of the active site of Cdc25A is known to be smaller than that of Cdc25B due to the differences in the positioning of the side chains of Met403 and Met488 in Cdc25A and those of the corresponding Leu445 and Met531 in Cdc25B.¹⁸ This is consistent with the results of the current docking simulations in which the terminal groups of **1e** and **2k** are situated deeper in the active site of Cdc25B than in that of Cdc25A. Despite the differences in the active site geometry and in the binding modes, the inhibitors appear to be stabilized in a similar way through the establishment of multiple hydrogen bonds and hydrophobic contacts with active-site residues of the two Cdc25 phosphatases.

Acknowledgment

This work was supported by the grant from KRIBB Research Initiative Program.

References and notes

- Kristjansdottir, K.; Rudolph, J. *Chem. Biol.* **2004**, *11*, 1043.
- Rudolph, J. *Biochemistry* **2007**, *46*, 3595.

- Galaktionov, K.; Lee, A. K.; Eckstein, J.; Draetta, G.; Meckler, J.; Loda, M.; Beach, D. *Science* **1995**, *269*, 1575.
- Takemara, I.; Yamamoto, H.; Sekimoto, M.; Ohue, M.; Noura, S.; Miyake, Y.; Matsumoto, T.; Aihara, T.; Tomita, N.; Tamaki, Y.; Sakita, I.; Kikkawa, N.; Matsuura, N.; Shiozaki, H.; Monden, M. *Cancer Res.* **2000**, *60*, 3043.
- Ngan, E. S. W.; Hashimoto, Y.; Ma, Z.-Q.; Tsai, M. J.; Tsai, S. Y. *Oncogene* **2003**, *22*, 734.
- Boutros, R.; Dozier, C.; Ducommun, B. *Curr. Opin. Cell Biol.* **2006**, *18*, 185.
- Fauman, E. B.; Cogswell, J. P.; Lovejoy, B.; Rocque, W. J.; Holmes, W.; Montana, V. G.; Piwnica-Worms, H.; Rink, M. J.; Saper, M. A. *Cell* **1998**, *93*, 617.
- Reynolds, R. A.; Yem, A. W.; Wolfé, C. L.; Deibel, M. R.; Chidester, C. G.; Watenpaugh, K. D. *J. Mol. Biol.* **1999**, *293*, 559.
- Contour-Galcerà, M.-O.; Sidhu, A.; Prévost, G.; Bigg, D.; Ducommun, B. *Pharmacol. Ther.* **2007**, *115*, 1.
- Ham, S. W.; Carr, B. I. *Drug Des. Rev.* **2004**, *1*, 123.
- Lazo, J. S.; Aslan, D. C.; Southwick, E. C.; Cooley, K. A.; Ducruet, A. P.; Joo, B.; Vogt, A.; Wipf, P. *J. Med. Chem.* **2001**, *44*, 4042.
- Sohn, J.; Kiburz, B.; Li, Z.; Deng, L.; Safi, A.; Pirrung, M. C.; Rudolph, J. *J. Med. Chem.* **2003**, *46*, 2580.
- Brault, L.; Denancé, M.; Banaszak, E.; Maadidi, S. E.; Battaglia, E.; Bagrel, D.; Samadi, M. *Eur. J. Med. Chem.* **2007**, *42*, 243.
- Huang, W.; Li, J.; Zhang, W.; Zhou, Y.; Xie, C.; Luo, Y.; Li, Y.; Wang, J.; Li, J.; Lu, W. *Bioorg. Med. Chem. Lett.* **2006**, *16*, 1905.
- Lazo, J. S.; Nemoto, K.; Pestell, K. E.; Cooley, K.; Southwick, E. C.; Mitchell, D. A.; Furey, W.; Gussio, R.; Zaharevitz, D. W.; Joo, B.; Wipf, P. *Mol. Pharmacol.* **2002**, *61*, 720.
- Lavecchia, A.; Cosconati, S.; Limongelli, V.; Novellino, E. *ChemMedChem* **2006**, *1*, 540.
- Park, H.; Carr, B. I.; Li, M.; Ham, S. W. *Bioorg. Med. Chem. Lett.* **2007**, *17*, 2351.
- Park, H.; Bahn, Y. J.; Jung, S.-K.; Jeong, D. G.; Lee, S.-H.; Seo, I.; Yoon, T.-S.; Kim, S. J.; Ryu, S. E. *J. Med. Chem.* **2008**, *51*, 5533.
- Shoichet, B. K.; Leach, A. R.; Kuntz, I. D. *Proteins* **1999**, *34*, 4.
- Wang, R.; Gao, Y.; Lai, L. *J. Mol. Model.* **2000**, *6*, 498.
- Wang, R.; Liu, L.; Lai, L. *J. Mol. Model.* **1998**, *6*, 379.
- Gasteiger, J.; Marsili, M. *Tetrahedron* **1980**, *36*, 3219.
- Kang, H.; Choi, H.; Park, H. *J. Chem. Inf. Model.* **2007**, *47*, 509.
- Morris, G. M.; Goodsell, D. S.; Halliday, R. S.; Huey, R.; Hart, W. E.; Belew, R. K.; Olson, A. J. *J. Comput. Chem.* **1998**, *19*, 1639.
- Lipinski, C. A.; Lombardo, F.; Dominy, B. W.; Feeney, P. J. *Adv. Drug Delivery Rev.* **1997**, *23*, 3.
- With respect to the numbering scheme for the amino acids, we followed those used in the X-ray crystallographic studies of Cdc25A (Ref. 7) and Cdc25B (Ref. 8).
- Tamura, K.; Southwick, E. C.; Kerns, J.; Rosi, K.; Carr, B. I.; Wilcox, C.; Lazo, J. S. *Cancer Res.* **2000**, *60*, 1317.
- Osada, S.; Osada, K.; Carr, B. I. *J. Mol. Biol.* **2001**, *314*, 765.